

Designing a Control System for Temperature Regulation in the Axiom HAB1

Isaiah Persad
Faculty of Mechanical Engineering
University of Sydney
Sydney, Australia
persad2016@gmail.com

Abstract—This document discusses the research and strategies to design a control system for heating the axiom HAB1. It focuses on the safety, efficacy and specific design requirements for a system in space. The thermal dynamics of the HAB1 are derived first-hand and a state space controller is created. Simulations and analysis of the close-looped responses are discussed. SI units are used throughout the entirety of this report.

I. INTRODUCTION

In this report, the research and strategies to design a temperature regulation system for a commercial space viewing pod are discussed in detail. With the increasing opportunities for commercialization in space travel, NASA has awarded contracts to private companies to develop their own modules for attachment to the ISS. Axiom has been awarded one of these contracts to create a central node module called the AxH1 or HAB1 [1]. The HAB1 is proposed to have a large window designed only for space viewing similar to the station's current Cupola Module [2]. The main objective of this report is to design an independent heating system for the HAB1 module that is separate from the main heating and cooling systems of the ISS. The ability to function autonomously is beneficial in the event of an emergency the system can be deactivated to save on power for essential systems, or used as a backup. The need for a separate control is evidenced by the pump failure incident in 2010, which required multiple spacewalks to repair. The secondary purpose and controller design goal of this report is to provide a heating system designed specifically to counteract the heat losses from windows. While the ISS orbits Earth it experiences significant temperature fluctuations, ranging from approximately 95°C when exposed to direct sunlight to around -130°C on the night side of Earth [3]. The HAB1 is a viewing POD, and the windows will be used primarily while the ISS is positioned on the night side of earth as the sun's radiation is harmful without protection. Passive methods include insulation, thermal coatings, and heat generated by onboard equipment, while the active thermal control system utilizes ammonia as a heat transport fluid. This report proposes integrating a separate control system native to the HAB1 module instead of incorporating the HAB1's dynamics into the existing ISS heating control system. The heating method used by ISS currently will be expanded on as ammonia heating is the current system and proven trustworthy. Ammonia was selected as it meets all of NASA's thermal

performance and safety requirements (toxicity, flammability, freeze temperature, stability, cost and successful commercial and industrial use) [3]. To design the controller for countering the heat loss through the HAB1 windows, the problem and HAB1 parameters are first defined. Using the constraints of the problem, Energy balances are derived to model the dynamics of thermal energy transfer, which are then related to the temperature inside the HAB1 module. The energy balances are linearized and the dynamics are represented by a state space model. Three controllers are designed and compared through closed loop validations to determine the most suitable for the HAB1. Disturbances and parameter variations are observed and analyzed for the selected controller. The findings are summarized in the conclusion.

II. SYSTEM DEFINITION

The intention of designing an additional controller in this report is not to address the cooling needs of the Axiom HAB1 but rather to specifically address the issue of heat loss through the module's large windows. Cooling requirements, if any, are not within the scope of this controller's design Figure 1

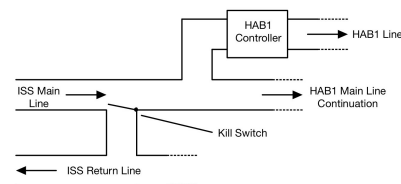


Fig. 1. Proposed Control System

illustrates the proposed configuration of the HAB1 heating system, which will be separate from the main ISS piping. As previously mentioned, an important feature of this system is the inclusion of a kill switch. The dimensions of the HAB1 can be determined from 2. The viewing window located at the end of the HAB1 will have the same diameter and will be constructed using high-temperature quartz glass to withstand the thermal cycling without cracking [5]. Standard ISS glass panels have 4 panes of class ranging from 1/2 to 1-1/4 inches thick [6]. For this controller the average thickness will be used as 0.1m. The hatch to enter the HAB1 will be made out of



Fig. 2. HAB1 Image [4]

steel and will have a diameter of 0.8128m with a thickness of 0.1587m to be compatible with existing ISS docking modules [7].

There are no previous dynamics to describe the HAB1, so they will be derived first hand. To achieve this, the quartz window, the air inside the HAB1, and the steel hatch will be considered as three separate control volumes. The equations describing the energy transfer will be functions of the temperature of the quartz glass (T), temperature of the control volume (T_i) and temperature of the ship (T_s). The system will also depend on the emissivity surface area (A_s), which represents the exposed surface area to space accounting for energy loss through the windows. In order to minimize energy loss through the windows, the ISS uses low emissivity exterior aluminum shutters to cover the emitting surfaces when they are not in use [6]. A_s will vary depending on the amount of the original surface area of the quartz glass that is uncovered. The controller can be physically described as the thermal energy generated within the control volume, which is sourced from the ammonia piping running through the HAB1. The efficiency of a pump can be described as $\eta = \frac{W_{in}}{W_{out}}$. The efficiency of a pump is influenced by factors such as the pressure difference along the piping, velocity difference, elevation difference, gravity, and frictional losses. In the context of space and assuming a steady incompressible flow, all factors except for frictional losses can be neglected. The main goal is to regulate the temperature of the system, the dynamics can be simplified by disregarding frictional losses caused by valves, fittings, elbows, and resistance. Therefore, the difference between the pump input power and output power ($W_{in} - W_{out}$) is equal to the thermal energy generation of the system, denoted as q_{gen} or u .

$$W_{in} - W_{out} = q_{gen} = u = \rho V c_{pA} \Delta T \quad (1)$$

By utilizing Equation 1, the input of the controllers to the energy balance can be defined as a reference temperature measured in watts.

A. Deriving System Model

The temperature of the air inside the HAB1 is affected by the transfer of thermal energy into and out of the system. To accurately model this energy transfer, multiple energy balances must be considered to account for the movement of thermal energy through different mediums. The the HAB1 is coated with insulators such as aluminized mylar. Aluminized mylar prevents solar radiation from escaping as it has a low emissivity of 0.044. It is assumed that the thermal energy

TABLE I
RELEVANT PROPERTIES OF CONTROL VOLUMES

Quartz Glass Control Volume		
Diameter	D_g	4.43 m
Thickness	T_g	0.1 m
Area (Adjoined with Control Volume)	A_g	15.41 m ²
Volume	V_g	1.56 m ³
Density	ρ_g	2200 kg/m ³
Specific Heat Capacity	c_{pg}	670 J/KgK
Convection Coefficient	h_g	6 W/m ² K
Thermal Conductivity	k_g	1.4 W/mK
Emmissivity	ϵ	0.6
Stephan Boltzmann Constant	σ	5.67 x 10 ⁻⁸ W/m ² K ⁴
Air Control Volume		
Diameter	D_a	4.43 m
Thickness	T_a	10.83 m
Volume	V_a	166.92 m ³
Density	ρ_a	1.225 kg/m ³
Specific Heat Capacity Air	c_{pa}	1000 J/KgK
Specific Heat Capacity Ammonia	c_{pA}	2200 J/KgK
Steel Hatch Control Volume		
Diameter	D_d	0.8128 m
Thickness	T_d	0.1587 m
Area (Adjoined with Control Volume)	A_d	0.5189 m ²
Volume	V_d	0.0823 m ³
Density	ρ_d	8050 kg/m ³
Specific Heat Capacity	c_{pd}	420 J/KgK
Convection Coefficient	h_d	13.4 W/m ² K
Thermal Conductivity	k	45 W/mK

lost to space through the mylar is negligible. Under this assumption, and considering that the surrounding area is a vacuum where conduction and convection do not occur, the remaining surfaces of the HAB1 can be treated as impermeable to heat transfer. A basic understanding of fluid mechanics and heat and mass transfer is assumed through the derivation. In 3

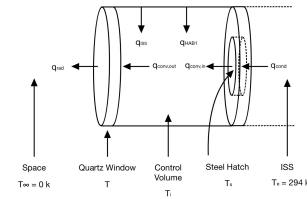


Fig. 3. Free Body Diagram of Heat Transfer

the free body diagram of the HAB1 heat transfer that occurs in each medium is shown

1) Energy Balance of Quartz Glass:

$$E_{in} - E_{out} + E_{gen} = E_{st}$$

The lumped capacitance method is used. This states that the temperature distribution is equal throughout the volume of the quartz glass if the Biot number is less than 0.1

$$Bi = \frac{h_g L_c}{K} < 0.1, L_c = \frac{V_g}{A_g}$$

$$Bi = \frac{(6)(1.56)}{(1.4)(15.41)} = 0.4$$

While the Biot number exceeds 0.1 a small temperature gradient could potentially exist in the quartz glass. However, since the Biot number remains low, we will continue to assume the lumped capacitance method.

Energy Stored in Quartz Glass with Lumped Capacitance Method:

$$E_{st} = \rho V c_p \frac{dT}{dt} = \rho_g V_g c_{pg} \frac{dT}{dt} \quad (2)$$

Energy entering the quartz glass volume through convection from air in the control volume:

$$E_{in} = q''_{in} = q_{conv,1} A = h A_g (T_i - T)$$

Assume convection coefficient h is uniform over surface, constant with time, thickness and height of glass

$$h = h_g, q_{conv,1} A = h_g A_g (T_i - T) \quad (3)$$

Energy leaving the quartz glass through radiation into space over the surface of emmissivity, as on the night side of earth only the emmissivity of radiation is considered:

$$E_{out} = q''_{out} = q_{rad} A = \epsilon \sigma A_s (T^4 - T_\infty^4)$$

Assume vacuum in space, $T_\infty = 0$

$$q_{rad} A = \epsilon \sigma T^4 A_s \quad (4)$$

Energy generation in the quartz glass control volume:

$$E_{gen} = \dot{q}_{gen} = 0$$

Final Energy Balance for quartz glass

$$\rho_g V_g c_{pg} \frac{dT}{dt} = h_g A_g (T_i - T) - \epsilon \sigma T^4 A_s$$

$$\dot{T} = \frac{1}{\rho_g V_g c_{pg}} [(h_g A_g) T_i + (-h_g A_g) T + (-\epsilon \sigma A_s) T^4] \quad (5)$$

2) Energy Balance Steel Hatch:

$$E_{in} - E_{out} + E_{gen} = E_{st}$$

The lumped capacitance is used again, assuming the temperature distribution is equal throughout steel door To use Lumped Capacitance $Bi < 0.1$

$$Bi = \frac{(13.4)(0.0823)}{(200)(0.5189)} = 0.0106 < 0.1$$

$$E_{st} = \rho V c_p \frac{dT}{dt} = \rho_d V_d c_{pd} \frac{dT_s}{dt} \quad (6)$$

Energy entering steel hatch comes from conduction due to the difference in temperature from the HAB1 to ISS. It is assumed that the ISS's temperature is kept constant at equilibrium of $T_e = 21^\circ\text{C} = 294\text{k}$ due to the proved efficacy of the ISS heating system.

$$E_{in} = q''_{in} = q_{cond} A = k A_d \frac{dT}{dx}$$

Temperature distribution is constant and linear through the steel door so the derivative function can be assumed as

$$\frac{dT}{dx} = \frac{T_e - T_s}{t_d - 0}$$

Energy out of the steel hatch volume to the air control volume through conduction

$$E_{out} = q''_{out} = q_{conv,2} A = h A_d (T_s - T_i)$$

Assume convection coefficient h is uniform and constant over time, thickness and height of glass

$$h = h_d, q_{conv,2} A = h_d A_d (T_s - T_i)$$

Energy generation in steel hatch volume

$$E_{gen} = \dot{q}_{gen} = 0$$

Final Energy Balance for the steel hatch

$$\rho_d V_d c_{pd} \frac{dT_s}{dt} = k A_d \frac{T_e - T_s}{T_d} - h_d A_d (T_s - T_i)$$

$$\dot{T}_s = \frac{1}{\rho_d V_d c_{pd}} [h_d A_d T_i + (-\frac{k A_d}{T_d} - h_d A_d) T_s + \frac{k A_d}{T_d} T_e] \quad (7)$$

3) Energy Balance for Control Volume:

$$E_{in} - E_{out} + E_{gen} = E_{st}$$

Without gravity, heat must be circulated manually within ISS modules. Assuming efficient air circulation and mixing throughout the module then temperature is uniformly distributed and remains constant throughout the space.

$$E_{st} = \rho V c_p \frac{dT}{dt} = \rho_a V_a c_{pa} \frac{dT_i}{dt} \quad (8)$$

Energy entering the control volume through convection from steel hatch and a constant thermal energy source from the main heating line of the ISS.

$$E_{in} = q''_{in} = q_{conv,2} A + q_{iss} = h_d A_d (T_s - T_i) + \dot{m} c_{pA} (T_s - T_i)$$

Energy leaves the control volume into the quartz glass via convection

$$E_{out} = q''_{out} = q_{conv,1} A = h_g A_g (T_i - T)$$

Energy generation from HAB1 control system

$$E_{gen} = \dot{q}_{gen} = \dot{q} V = V_a u$$

Final Energy Balance of control volume

$$\rho_a V_a c_{pa} \frac{dT_i}{dt} = h_d A_d (T_s - T_i) + \dot{m} c_{pA} (T_s - T_i) - h_g A_g (T_i - T) + V_a u$$

$$\dot{T}_i = \frac{1}{\rho_a V_a c_{pa}} [(-h_d A_d - \dot{m} c_{pA} - h_g A_g) T_i$$

$$+ (h_g A_g) T + (h_d A_d + \dot{m} c_{pA}) T_s + V_a u]$$

B. Linearization

The energy balance equation for quartz glass is non-linear due to relationship between radiation and surface temperature. For small perpetuation's in temperature, the equation can be linearized around the equilibrium point. Using a Taylor series expansion the system can be linearized for controller design. Taylor Series Expansion:

$$q_{rad}(T) = f(T) = f(T_e) + \frac{df}{dt}(T - T_e)$$

The point will be linearized around room temperature $T_e = 294k$

$$\begin{aligned} f(T_e) &= \epsilon\sigma A_s T_e^4, \quad \frac{df}{dt} = 4\epsilon\sigma A_s T_e^3 \\ q_{rad}(T) &= \epsilon\sigma A_s T_e^4 + 4\epsilon\sigma A_s T_e^3(T - T_e) \\ q_{rad}(T) &= 4\epsilon\sigma A_s T_e^3 T - 3\epsilon\sigma A_s T_e^4 \end{aligned} \quad (9)$$

The updated energy balance for the quartz glass volume is now:

$$\dot{T} = \frac{1}{\rho_g V_g c_{pg}} [(h_g A_g) T_i + (-h_g A_g - 4\epsilon\sigma A_s T_e^3) T + 3\epsilon\sigma A_s T_e^4] \quad (10)$$

C. State Space Model

Energy Balance Control Volume

$$\begin{aligned} a_{11} &= \frac{1}{\rho_a V_a c_{pa}} (-h_d A_d - \dot{m} c_{pA} - h_g A_g), \quad a_{12} = \frac{1}{\rho_a V_a c_{pa}} (h_g A_g) \\ a_{13} &= \frac{1}{\rho_a V_a c_{pa}} (h_d A_d + \dot{m} c_{pA}), \quad b_{11} = \frac{1}{\rho_a c_{pa}} \\ \dot{T}_i &= a_{11} T_i + a_{12} T + a_{13} T_s + b_{11} u \end{aligned}$$

Energy Balance Quartz Glass

$$\begin{aligned} a_{21} &= \frac{1}{\rho_g V_g c_{pg}} (h_g A_g), \quad a_{22} = \frac{1}{\rho_g V_g c_{pg}} (-h_g A_g - 4\epsilon\sigma A_s T_e^3) \\ d_{21} &= \frac{1}{\rho_g V_g c_{pg}} (3\epsilon\sigma A_s T_e^4) \\ \dot{T} &= a_{21} T_i + a_{22} T + d_{21} \end{aligned}$$

Energy Balance Steel Door

$$\begin{aligned} a_{31} &= \frac{1}{\rho_d V_d c_{pd}} h_d A_d, \quad a_{33} = \frac{1}{\rho_d V_d c_{pd}} \left(-\frac{k A_d}{T_d} - h_d A_d\right) \\ d_{31} &= \frac{1}{\rho_d V_d c_{pd}} \left(\frac{k A_d T_e}{T_d}\right) \\ \dot{T}_s &= a_{31} T_i + a_{33} T_s + d_{31} \end{aligned}$$

The derived equations can be put into state space form with 1 output, 1 input, and 3 states. It is described by the dimensional state vector x , output y , input u , coefficient matrices A & B & C , and disturbance matrix d .

$$\begin{aligned} \frac{d}{dt} \begin{bmatrix} T_i \\ T \\ T_s \end{bmatrix} &= \begin{bmatrix} a_{11} & a_{12} & a_{13} \\ a_{21} & a_{22} & 0 \\ a_{31} & 0 & a_{33} \end{bmatrix} \begin{bmatrix} T_i \\ T \\ T_s \end{bmatrix} + \begin{bmatrix} b_{11} \\ 0 \\ 0 \end{bmatrix} u + \begin{bmatrix} 0 \\ d_{21} \\ d_{31} \end{bmatrix} \\ y &= [1 \ 0 \ 0] x \end{aligned}$$

In 4 the state space system, is modeled in simulink.

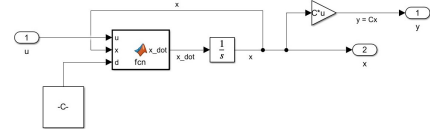


Fig. 4. State Space Model

III. CONTROLLER DESIGN

A. Controller goals

The effectiveness of the controller will be analyzed on its ability to track and keep a reference temperature for astronauts comfort. The standard reference temperature is room ($T_e = 21^\circ = 294k$). The controller's performance will be tested by examining its capability to heat the HAB1 from an initial temperature of 283 K for all system states. The design of the controller is subject to various constraints imposed by the problem, including timing, passenger comfort, and energy usage. The design of the controller is limited by the constraints of the problem, including timing, comfort of passengers and energy usage. The ISS orbits earth 90 times a day, spending 45 mins in the light and 45mins in the dark, limiting the run time to 2700s. To maximize the time available for viewing the settling time of the controller will be 10mins or 600s. The damping of the system is chosen from the desired overshoot of the controller. In this application overshoot is an important constraint as the temperature should remain comfortable and habitable in the ISS at all times. To keep the temperature range from a maximum 0-40 degrees Celsius and overshoot of 10% is deemed acceptable. The correlates to a damping ratio of 0.6.

B. Full-state Feedback Controller

For the state feedback controller, all the states must be measured to have the necessary information to determine the control input. The systems controllability is determined through the rank of the controllability matrix $w = [B \ AB \ A^2B \dots]$. For the HAB1 this can be found by using the `ctrb` and `rank` functions in matlab. The HAB1 state space models controllability has full rank, so then through design of the controller the poles can be moved. The control input takes the form $u = -Kx + k_r r$. Figure 5 can be used with a matlab script

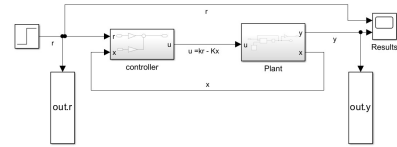


Fig. 5. Full-State Feedback Controller Model

to run the closed loop dynamics of the HAB1 with state gain K_s and feed-forward gain k_r . The state gain $u = K_s x$ can be found with the new closed loop system

$$\dot{x} = (A - BK)x + Bk_r r$$

Knowing for A in reachable canonical form there holds

$$\det(sI - A) = s^3 + a_1s^2 + a_2s + a_3$$

Then A-BK in reachable canonical is

$$\det(sI - A) = s^3 + (a_1 - k_1)s^2 + (a_2 - k_2)s + (a_3 - k_3)$$

The desired characteristic polynomial is

$$G_{desired}(s) = (s + N\delta W_n)(s^2 + 2\delta W_n s + W_n^2)$$

The two second order dominant poles are chosen based on the desired transient response.

$$p(s) = (s^2 + 2\delta W_n s + W_n^2)$$

The system has three states so a third pole is placed, with the real part of the pole further left. This results in a faster settling time described by N. For the HAB1 system, N = 5

$$(s + N\delta W_n)$$

By putting the desired characteristic polynomial under reachable form

$$(s + N\delta W_n)(s^2 + 2\delta W_n s + W_n^2) = s^3 + p_1s^2 + p_2s + p_3$$

The state gain can be obtained as $k_i = p_i - a_i$. Subbing in the parameters

$$K = [k_1 \ k_2 \ k_3] = [0.45 \ 0.051 \ 0.0028]$$

The reachability matrix for the canonical form can be found as $w_t = [1 \ * \ *; 0 \ 1 \ *; 001]$. It is used to find the transformation T. Knowing that if $z = Tx$ with T invertable the state space model becomes

$$\dot{z} = A_t z + B_t u \quad (11)$$

Now that state feedback $u = Kz$ is set equal to $u = KTx$ to find the state feedback.

$$T = W_t W^{-1}, \quad u = KTx$$

Lastly, the feed-forward gain is found by setting the full closed loop system to a constant reference. Knowing from that the system is stable.

$$y_{ss} = Cx_{ss} = -C(A - BK)^{-1}Bk_r$$

$$k_r = \frac{-1}{C(A - BK)^{-1}B} = 4.37$$

In 6 the dynamics of the controller are simulated starting with the initial conditions of all states at 283K. In the time simulated (45mins = 2700s) the controller did not converge to the reference temperature of 294k and exhibited large steady state error. The controller instead converges to 288.84 k with a settling time of 4184 seconds. To analyze the source of the error the controller was first double checked for proper design. This was done by running 5 with proven values from literature. The stability of the system dynamics was observed, and no inherently unstable or oscillatory behavior was found. The system has no noise, and had no saturation constraints. Manual tuning of the controller was attempted, but no combination of the gain values K_s and k_r resulted in satisfactory convergence to the reference temperature.

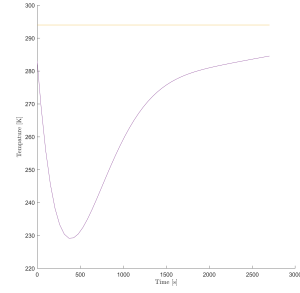


Fig. 6. Closed loop Response of Full-state Feedback Controller

C. Full-State Feedback Controller with Integrator

The full-state controller with feed-forward and state gain had considerable steady-state error. To solve this issue an integrator is added to the system. When combined in series with the plant, the steady state error due to the step reference can be mitigated. The cost of adding an integrator is increasing the number of states in the model by one. This changes the control structure of the full-state model. The augmented state equations with the extra state for the integral of the error is

$$\frac{d}{dt}[x \ z] = [A \ 0; \ C \ 0][x \ z] + [B; \]u + [0; \ -1]r$$

The reference now does not affect any state but the integrator state or output of the plant as there is no path from the reference to the plant input u without implementing the state gain matrix K_s . The integral of the error is fed back and reduces the steady state error to zero. To redesign the controller to account for the augmented state, the pole associated with the integrator state will be moved $N=10$, so its settling time is faster than the other poles. The same procedure as the full-state without integral control is applied to find the state gains K_s and integral gain K_i through coefficient matching. In 7 the

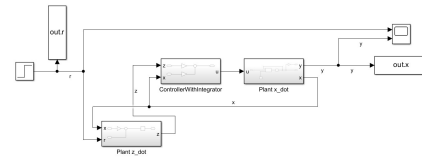


Fig. 7. Full State with integrator Controller

new controller with an integrator is modeled in simulink. In 9, the closed-loop response of the system with the full-state integral controller is presented, aiming to heat the HAB1 to the reference temperature of 294 K starting from initial conditions of all states at 283 K. It is noted that the addition of integral control has brought in oscillations to the system hinting that the integral control may be dominating the control signal. The steady state error of the system is eliminated only when the controller is given longer that 2700s to converge. This is not suitable for the purpose of the HAB1 as a slow settling time has no benefit for passengers viewing space. Similar to

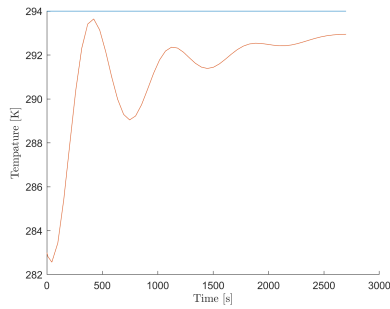


Fig. 8. Full State with integrator Controller Closed Response

previous analyses, the system was examined for any potential errors, but none were identified. Consequently, the gains of the full-state integral controller were tuned in an attempt to achieve more desirable performance.. In 9, 10, and 11, the

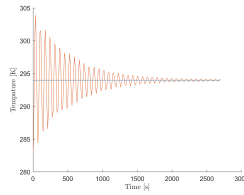


Fig. 9. High K_i & original K_s for Full State Integrator Controller

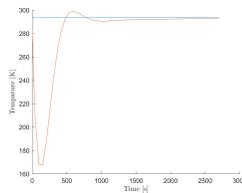


Fig. 10. Original K_i & High K_s for Full State Integrator Controller

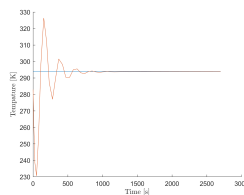


Fig. 11. High K_i & High K_s for Full State Integrator Controller

impacts of manually tuning the integral gain (K_i) and state gain (K_s) are analyzed in relation to the closed-loop response of the system described in 7. It is observed that increasing the integral gain leads to a reduction in steady-state error but an increase in oscillations in the response. This behavior is expected since higher integral gains amplify the accumulated error, resulting in more pronounced oscillations and a more aggressive response. Conversely, lower integral gains result in less oscillation but may lead to higher steady-state error.

Furthermore, the effects of higher state gain are demonstrated to decrease the settling time of the system, which is desirable for faster convergence. However, this comes at the expense of an increased amplitude of the overshoot in the response. Considering the specific use and purpose of the controller in

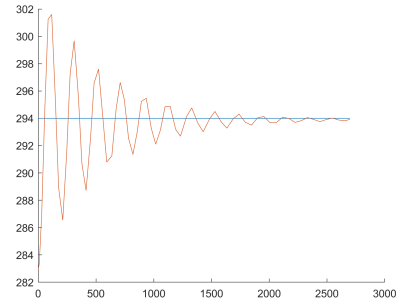


Fig. 12. Best Gains for Full State with integrator Controller

the HAB1, it has been determined that the combination of gains shown in 12 is the most suitable. By using 0.3 times the integral gain (K_i) and 300 times the state gain (K_s), a desirable settling time and minimal overshoot are achieved. Although gains closer to those shown in 10 may result in a cleaner signal and a more stable response, the higher overshoot in that case would require more correction to the temperature, which could be more noticeable and potentially uncomfortable for the passengers. On the other hand, the small oscillations observed in 12 are expected to have a lesser impact on the passengers' experience.

D. Output-Feedback Controller

When all the state variables cannot be measured, an observer can be used to estimate them. For the case of the HAB1 this could be very helpful as there then no need to implement sensors to the quartz window and steel door to measure the temperatures. The observer essentially replicates the plant with the same inputs and nearly identical dynamics. An additional term compares the actual measured output (y) to the estimated output, helping to correct the estimated state towards the true state values. The error dynamics are determined by the eigenvalues of the matrix $(A-LC)$, where L is the observer gain matrix. The addition of an observer in the output feedback controller means that a third gain matrix L needed to be brought into the equation. Because of the duality between controllability and observability, the same technique used to find the control matrix for the full-state observers can be used by replacing the coefficient matrix B with the coefficient matrix C in its place. This is the separation principle. To choose the observe to gain L , the poles are again placed $N=5$ times farther away from the two dominant poles of the system. 13 shows the structure of the observer, and how its a state estimator that balances the predictions based on the model and new information arriving to the measurement. In the simulation shown in 15, the output-feedback closed-loop dynamics of the system and observer are analyzed when starting

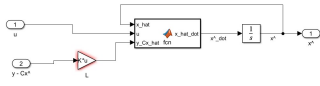


Fig. 13. Observer

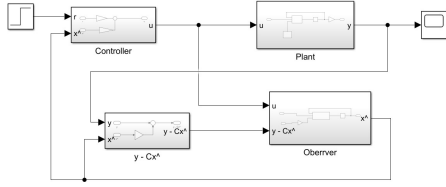


Fig. 14. Output-Feedback Controller

from an initial condition of 283K for all states. The observer showed that it could meet the settling time specification and converge to the reference but could not overcome the problem of the overshoot. The idea of the observer is that even with some unknown measurement noise and system disturbances, it should still produce a good estimate, but this may not always be the case. In the context of the HAB1's thermal dynamics and energy balance, disturbances are inherently present in the system from the beginning. The disturbances can introduce errors in the observers estimation, corrupt the measurements and lead to inaccurate state estimation and sub-optimal control actions. If the disturbance is significant and is incorrectly estimated this may lead to the excessive response resulting in large overshoot.

IV. CLOSED LOOP VALIDATIONS

A. Controller Comparisons

When picking which controller best suits the HAB1, the full-state with integrator and output controller will be compared. The full-state with feedback controller exhibited too much steady state error to be considered. So far the controllers designed for the HAB1 have been observed through general speculation of close-loop response. In 16 the response of

TABLE II
COMPARISON OF INTEGRATOR VS. OBSERVER

Feature	Integrator	Observer
Settling Time (s)	140	686
Overshoot Value (k)	301.6	143.4
Overshoot difference (k)	7.6	151

the two controllers are plotted against each other and the numerical response specifications are observed in II. The settling time refers to the time the system takes to reach a stable state or to settle within an acceptable range of $\pm 1k$. The overshoot value describes the maximum deviation from the reference value and the overshoot difference is the difference between the maxim deviation and reference values. Although experiencing slight steady state oscillation due to the integral

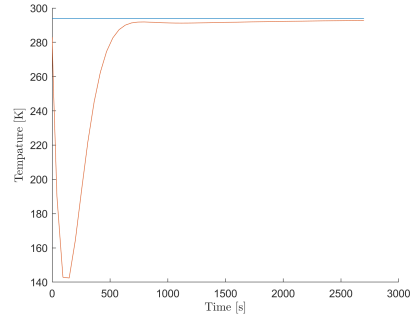


Fig. 15. Output-feedback Controller with with closed loop dynamics

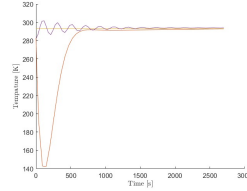


Fig. 16. Comparison of Integrator and Observer

gain, the full state integral controller fits the design constraints for the HAB1 heating better than the observer. Its settling time and overshoot are well within 600s and 10% respectively.

B. Additional Disturbances

The HAB1 will not be an empty control volume in practicality. Its main purpose is to provide a viewing area, which will be inhabited by humans. This will add an additional disturbance to the system as humans give off an average of 100W per hour. For a cycle of 45 mins that is 75W per human. The disturbance will be modeled as 5 astronauts in the room for a total extra energy generation of 375W. Adding this disturbance to the air control volume moves it to the d matrix.

$$d = \begin{bmatrix} d_{11} \\ d_{21} \\ d_{31} \end{bmatrix}, d_{11} = \frac{1}{\rho_a V_a c_{pa}} \rho V c_p \Delta T$$

Comparing 17 to 7 it is noted that the disturbance decreases

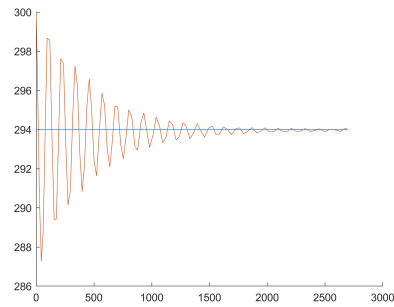


Fig. 17. Additional Disturbance with humans

the overshoot from 301.6 to 299.9k and moves the settling

time up to 133.3 seconds. This is to be expected, the goal of the control is to heat the HAB1, with the human disturbance it aids the controller, helping it increase the temperature of the control volume from 283 to 294k faster.

C. Variable Parameters

The main feature that sets the HAB1 different from other modules in the ISS is its large window, and one of the controllers goals is to independently keep the room at a reference temperature despite the energy lost through radiation out of the high emissivity glass. The sliding aluminum mylar covers over the quartz window and the remaining surface area exposed is A_s . Its values will be $0.1A_g$, $0.25A_g$, $0.5A_g$, $0.75A_g$. The value of A_s does not affect the volume or surface area A_g , it is simply the amount of window uncovered by solar protection. To validate the controllers usage for the window the area of emissivity can be changed and the response of the controller observed. In III the overshoot and settling times

TABLE III
EFFECT OF AREA OF EMISSIVITY ON HAB1 HEATING CONTROLLER

A_s	Overshoot	Settling time
$0.75A_g$	299.7	133.8
$0.5A_g$	298.0	120.0
$0.25A_g$	296.9	105.4
$0.1A_g$	295.6	85.55

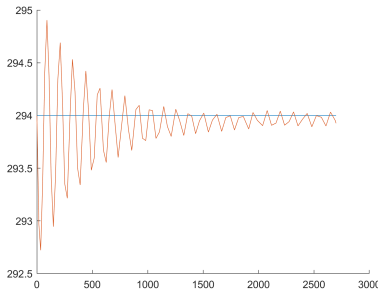


Fig. 18. Full-state with Integrator and $A_s = 0.1A_g$

of the system as a function of the area of emissivity are observed. In order to isolate the effect, the initial condition was changed from 283 k to an ambient 294. In 18 the response of the controller with the window area at 10% of its original value is shown to have a settling time of just over one minute and an overshoot of 1.1 k. With a smaller exposed area, the controllers require less corrective action to counterbalance the heat loss or gain. As a result, the overshoot and settling time of the controllers would decrease. This behavior aligns with the intuition that a smaller surface area for heat transfer would lead to a more stable and responsive control system.

V. CONCLUSION

In this report, three controllers were designed and compared to track a reference temperature for the Axiom HAB1. To accomplish this, the thermal dynamics of the HAB1 were

modelled, and the performance of the three controllers was evaluated through closed-loop validations. Among the three controllers, the recommended choice for the HAB1 was a full-state controller with an integrator. This controller met the settling time and overshoot goals from the desired response specifications. To meet the design criteria the gains of manually tuning was performed. The result of manual tuning resulted in the domination of the control signal from the integral gain, leading to heavy oscillation around the reference. To improve on the controller design it would be beneficial to test the controller using nonlinear dynamics that consider the HAB1's cooling through radiation and incorporate a time delay to account for the temperature gradient within the HAB1. Incorporating a time delay was beyond the scope of the current study and would require further knowledge from advanced design courses. Additionally, it would be advantageous to evaluate a time-based signal that gradually decreases from when the HAB1 enters the night side, as this would provide a more accurate representation of the system's behaviour in the absence of step references, assuming the heater performs its function effectively. However, the designed controller still had room for improvement to meet the standards of the ISS. It is recommended that in further study the dynamics are remodelled and an output-feedback controller tested further. The assumption of no frictional losses and energy loss through the walls of the HAB1 may have greater effects on the controller than anticipated. Despite the presence of low emissivity fillers lining the walls of the HAB1, the cumulative surface area might be significant enough to render their effect non-negligible. While the full-state feedback controller is effective, its implementation on the ISS is impractical due to the requirement of having a large number of sensors corresponding to the system states. In summary, the full-state integral controller design successfully met the desired criteria. However, it is strongly recommended to remodel the dynamics to address the issues related to the output feedback controller to improve its performance.

REFERENCES

- [1] Axiom commercial space station. Axiom Space. (n.d.). <https://www.axiomspace.com/axiom-station>
- [2] J. O'Callaghan, "The ISS is getting an extension - which might detach and form its own commercial space station," *Forbes*, <https://www.forbes.com/sites/jonathanoconnor/2020/01/28/the-iss-is-getting-an-extension-which-might-detach-and-form-its-own-commercial-space-station/> (accessed May 28, 2023).
- [3] J. Wright, "Cooling system keeps space station safe, productive," NASA, <https://www.nasa.gov/content/cooling-system-keeps-space-station-safe-productive> (accessed May 28, 2023).
- [4] B. Wang et al., "Axiom space station," *NextBigFuture.com*, <https://www.nextbigfuture.com/2021/06/axiom-space-station.html> (accessed May 28, 2023).
- [5] B. Dunbar, "Spacecraft Design," NASA, <https://www.nasa.gov/centers/ames/research/2007/faqshuttleclass.html> (accessed May 28, 2023).
- [6] "Home, space home," NASA, <https://science.nasa.gov/science-news/science-at-nasa/2001/ast14mar1/> (accessed May 28, 2023).
- [7] "NASA marshall space flight center human factors engineering analysis of various hatch sizes - NASA technical reports server (NTRS)," NASA, <https://ntrs.nasa.gov/citations/20190030368> (accessed May 28, 2023).

**See comments for information on simple extension